Spin-orbital liquid in $Ba_3CuSb_2O_9$ stabilized by oxygen holes

Kou Takubo,[1,2] Huiyuan Man,[1,3] Satoru Nakatsuji,[1,3,4] Kohei Yamamoto,[1] Yujun Zhang,[1] Yasuyuki Hirata,[1] Hiroki Wadati,[1,5] Akira Yasui,[6] Takashi Mizokawa,[7] and Daniel I. Khomskii[8]

[1]*Institute for Solid State Physics, University of Tokyo, Kashiwa, Chiba 277-8581, Japan*
[2]*Department of Chemistry, Tokyo Institute of Technology, Meguro, Tokyo 152-8551, Japan*
[3]*Institute for Quantum Matter and Department of Physics and Astronomy, Johns Hopkins University, Baltimore, Maryland 21218, USA*
[4]*Department of Physics, University of Tokyo, Hongo, Tokyo 113-0033, Japan*
[5]*Department of Material Science, University of Hyogo, Ako, Hyogo 678-1297, Japan*
[6]*Japan Synchrotron Radiation Research Institute (JASRI/SPring-8), Sayo, Hyogo 678-1297, Japan*
[7]*Department of Applied Physics, Waseda University, Okubo, Tokyo 277-8581, Japan*
[8]*II Physikalisches Institut, Universität zu Köln, Zülpicher Strasse, 50937 Cologne, Germany*

(Received 23 March 2021; accepted 1 July 2021; published 19 July 2021)

We report x-ray and optical absorption spectroscopy as well as hard x-ray photoemission spectroscopy on hexagonal $Ba_3CuSb_2O_9$ in which a Cu 3*d* spin-orbital liquid state is suggested from absence of the Jahn-Teller distortion of $Cu^{2+}O_6$ octahedra and of the magnetic ordering. The experimental results and their cluster model analysis indicate that O 2*p* holes play a crucial role in realizing the spin-orbital liquid state of hexagonal $Ba_3CuSb_2O_9$. These oxygen holes appear due to the "reaction" $Sb^{5+} \rightarrow Sb^{3+}$ + two O 2*p* holes, with these holes being able to attach to Cu ions. The present work opens avenues towards spin-charge-orbital entangled liquid state in transition-metal oxides with small or negative charge transfer energy.

DOI: 10.1103/PhysRevMaterials.5.075002

I. INTRODUCTION

Ligand holes, e.g., oxygen holes often present in oxides with, typically, high valence (or high oxidation state) of metals (such as nominally Fe^{4+} in $CaFeO_3$ [1], Cu^{3+} in $NaCuO_2$ [2] or Bi^{4+} in $BaBiO_3$ [3,4]) lead to various nontrivial effects, which largely determine the properties of corresponding solids [5,6]. The oxygen holes provide a novel type of up-up-down-down magnetic structure of RNiO$_3$ (R = rare earth ions [7], spontaneous charge or rather valence bond disproportionation in $CaFeO_3$ [1] and $BaBiO_3$ [3,4]. In addition, oxygen holes apparently play fundamental roles in high-T_c superconductivity in cuprates (presumably connected with the formation of Zhang-Rice singlets [8]). In the present work, we study electronic structure of hexagonal $Ba_3CuSb_2O_9$ in order to uncover yet another nontrivial effect due to the presence of oxygen holes: the suppression of Jahn-Teller (JT) distortion and magnetic ordering, typical for the strong JT ion Cu^{2+}, with the resulting formation of spin-orbital liquid state in a very interesting material $Ba_3CuSb_2O_9$ [9]. We also show that, besides the suppression of the JT and magnetic ordering, oxygen holes lead to a very specific dynamic effects.

The octahedrally coordinated Cu^{2+} with $3d^9$ electronic configuration (one hole in the ten-fold Cu 3*d* subshell) is known as one of the classical JT active ions. Usually, divalent CuO_6 octahedron in concentrated systems always leads to a cooperative orbital ordering with the concomitant lattice distortion (cooperative JT effect; see, e.g., Refs. [10,11]). When the CuO_6 octahedron is elongated along the z-axis, the Cu 3*d* orbital with $x^2 - y^2$ symmetry is destabilized and accommodates the Cu 3*d* hole. $Ba_3CuSb_2O_9$ harbors orthorhombic phase [12] and hexagonal phase [9,13]. A very unusual and unexpected effect, the absence of JT distortion in a classical strong JT ion Cu^{2+} in octahedral coordination, was discovered in the hexagonal $Ba_3CuSb_2O_9$ by Nakatsuji *et al* [9]. There are very convincing experimental indications of a dynamic character of the behavior of Cu in this system [14,15]. Theoretically, quantum spin liquids are expected if the orbitals are fluctuating [16–19]. However, the real microscopic origin of this behavior was not elucidated in these detailed studies. The usual dynamic JT effect is unlikely since it is very rare in concentrated systems with some exceptions in 4*f* systems such as PrO_2 [20]. The dynamic JT effect is usually realized in well-isolated JT centers and never realized in concentrated 3*d* systems including Cu^{2+} oxides. An extra puzzle is that the same material seems to exist in two different modifications. The orthorhombic phase behaves quite normally: it shows a cooperative JT distortion, no special dynamic effects, etc. On the other hand, the hexagonal phase has all these strange features discussed above. The question "what is the microscopic reason for this very different behavior" remains a puzzle.

Here we present experimental results which shed light on this question and which give us the possibility to solve all these puzzles. Notably, the x-ray absorption spectroscopy (XAS) on $Ba_3CuSb_2O_9$ shows that, whereas the orthorhombic phase contains the usual Cu^{2+} with all the conventional features thereof, in the hexagonal phase we see definite signatures of the presence of substantial oxygen hole character. Fluctuations, inevitably appearing due to motion of these

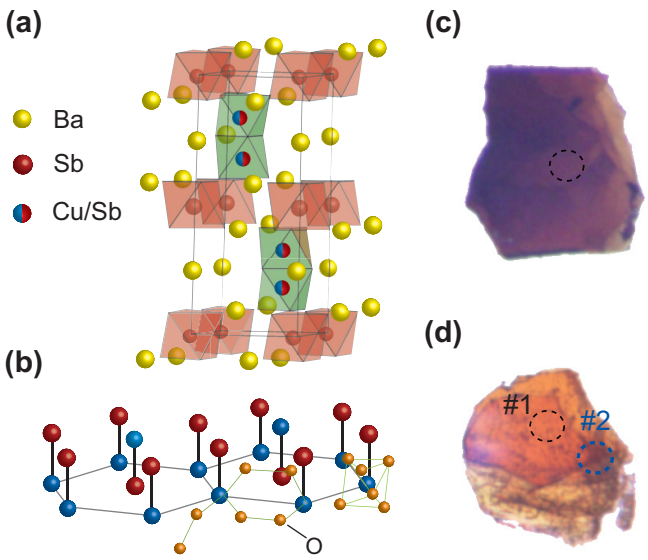

FIG. 1. (a) Crystal structure of hexagonal $Ba_3CuSb_2O_9$. The occupancy of Cu and Sb in the two metal sites of the Cu-Sb face-sharing dumbbells is 50%. (b) Short-range honeycomb lattices in the *ab* plane. (c, d) Sample photographs of hexagonal and orthorhombic samples. The thicknesses of both samples are below 5 μm. The dashed circles ($\phi \sim 50\,\mu$m) correspond to the selected regions for the optical absorption microscopy of Fig. 2(a).

oxygen holes hopping from site to site, suppress conventional long-range JT ordering and magnetic ordering and cause the dynamics seen in ESR and NMR [14,15].

The basic crystal structure of hexagonal $Ba_3CuSb_2O_9$ is shown in Fig. 1(a) (symmetry $P6_3/mmc$). Sb ions occupy the isolated octahedra and half of the octahedra forming face-sharing dimers [9,13]. Cu ions occupy the other half of the dimer octahedra. The Cu ions have short range order forming the honeycomb structure in the *ab*-plane as shown in Fig. 1(b). In orthorhombic $Ba_3CuSb_2O_9$ (symmetry *Cmcm*), the hexagonal structure of Fig. 1(b) becomes long ranged, and the CuO_6 octahedra are strongly distorted due to JT effect typical for Cu^{2+}.

II. METHODS

Single crystals of hexagonal $Ba_3CuSb_2O_9$ were grown under oxygen atmosphere from the $BaCl_2$-based flux with 9 mol % $Ba(OH)_2$ and are stoichiometric in terms of the Sb/Cu and Ba/Cu elemental ratios [13]. While the Sb/Cu elemental ratio is 2.0 in the hexagonal crystals, it is about 2.1 in the orthorhombic $Ba_3CuSb_2O_9$ crystals grown from the pure $BaCl_2$ flux [13]. A Fourier transform infrared spectroscopy microscope (JASCO IRT-30) was used for the optical microscopic measurements in the transmission mode. The space resolution was $\sim$30 μm. The optical absorption was estimated from the transmission. X-ray absorption spectroscopy (XAS) for the Cu L ($2p$) and O K ($1s$) core levels were performed using the surface-sensitive total electron yield (TEY) and bulk-sensitive total fluorescence yield (TFY) modes at BL07LSU in SPring-8 [21]. Hard x-ray photoemission spectroscopy (HAXPES) was performed at SPring-8 BL47XU. The photon energy was 7940 eV. The binding energy was calibrated by the Fermi edge of gold and the energy resolution was approximately 200 meV.

III. RESULTS AND DISCUSSION

An obvious difference between the hexagonal and orthorhombic phases is the "color" of the crystals. The crystal with dark color [Fig. 1(c)] is dominated by the hexagonal phase while the yellowish color crystal [Fig. 1(d)] mainly contains the orthorhombic phase. Figure 2(a) shows the optical absorption spectra for the hexagonal and orthorhombic crystals. The orthorhombic crystals exhibit inhomogeneity. The spectrum taken at position no. 1 [see Fig. 1(d)] represents the orthorhombic phase with optical gap $h\nu \sim 2.0$ eV, which corresponds to the oxygen $2p$ to Cu $3d$ charge transfer excitation as expected in Cu^{2+} oxides. On the other hand, the spectrum at position no. 2 exhibits an intriguing absorption centered around 1.3 eV ($\sim$950 nm) below the charge transfer excitation $\sim$2.0–3.0 eV. The appearance of the absorption peak in the charge transfer gap suggests that some holes are introduced in the Cu^{2+} Mott insulating state, similar to the high-T_c cuprates. Surprisingly, in the absorption spectrum for the hexagonal phase, the in-gap absorption peak around 1.3 eV gains substantial spectral weight which causes the dark color. This indicates that a considerable number of holes are doped in the hexagonal phase although it is highly insulating. The measured single crystals were grown with special care following the methods reported in Ref. [13]. The hexagonal crystals with doped holes are stoichiometric with the Sb/Cu ratio of 2.0. On the other hand, the orthorhombic crystals exhibit the Sb/Cu ratio of 2.1. Since the hexagonal and orthorhombic crystals are highly insulating, hole doping due to excess oxygen is unlikely. If the localized oxygen holes in the hexagonal crystals are provided by the self doping between Cu and Sb, 5% replacement of Cu^{2+} ions by Sb^{5+} ions can reduce 0.15 holes per Cu site in the orthorhombic crystals. Therefore, the self-doping mechanism would be consistent with the experimental results on the resistivity and the Sb/Cu ratio. In addition, the inhomogeneity of the orthorhombic crystals would be related to the offstoichiometry of the Sb/Cu ratio.

In order to further clarify this electronic structure difference between the hexagonal and orthorhombic phases, x-ray absorption spectroscopy have been performed for the two phases. Figure 2(b) shows the Cu $2p$ XAS spectra in the total fluorescence yield mode. The Cu $2p$ main peak at 930.2 eV is accompanied by the charge transfer satellite at about 933 eV. The intensity of the satellite is enhanced in the hexagonal phase compared to the orthorhombic phase. The main and satellite peaks are assigned to the transitions of $2p^63d^9 \rightarrow 2p^53d^{10}$ and of $2p^63d^9L \rightarrow 2p^53d^{10}L$ [2]. Here L represents a hole on the oxygen $2p$ orbitals. The Cu $2p$ XAS indicates that the ground state of the hexagonal phase includes more $3d^9L$ than the orthorhombic phase. Figure 2(c) shows the Cu $2p$ XAS spectra taken in the total electron yield mode. The XAS spectra in the total electron yield mode are more surface sensitive than those in the total fluorescence yield mode. The XAS results obtained in the two modes are very consistent indicating that the contribution of $3d^9L$ is not due to the surface effect. In the hexagonal phase, the intensity of

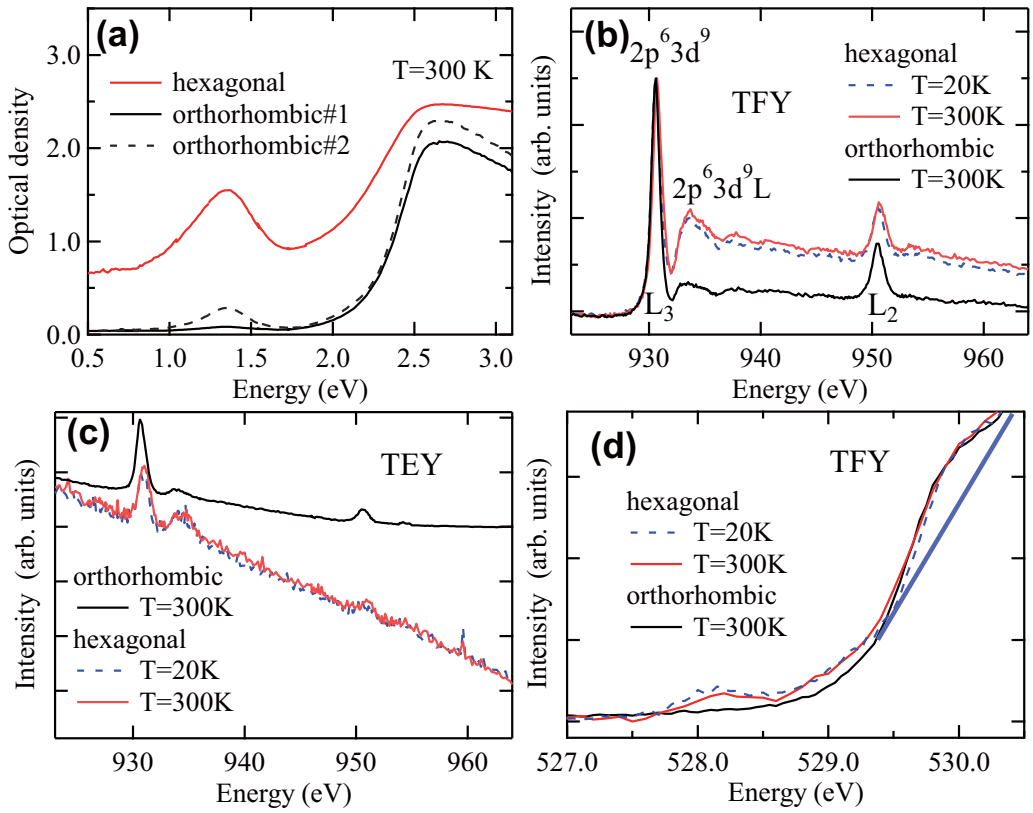

FIG. 2. (a) Typical optical absorption of the hexagonal and orthorhombic phases estimated from their transmission, which are taken in the transmission microscopy mode with space resolution of 30 μm. (b) Typical Cu $2p$ XAS spectra of the hexagonal and orthorhombic phases taken in the total fluorescence yield mode. (c) Typical Cu $2p$ XAS spectra of the hexagonal and orthorhombic phases taken in the total electron yield mode. (d) Typical O $1s$ XAS spectra of the hexagonal and orthorhombic phases taken in the total fluorescence yield mode.

the satellite is comparable to that of the main peak indicating that the oxygen hole concentration is about 1/6 [22]. This estimation of the oxygen hole concentration for the hexagonal system is consistent with the difference of the Cu/Sb ratio between the hexagonal and orthorhombic systems since the 5% replacement of Cu by Sb in the orthorhombic system can remove 0.15 holes from the Cu site.

Figure 2(d) shows the O $1s$ XAS spectra of the hexagonal and orthorhombic systems. The structure at 530 eV can be assigned to the transition from O $1s$ to O $2p$ hybridized into the upper Hubbard band (corresponding to $3d^9 \rightarrow 3d^{10}$). The peak at 528.2 eV is observed only in the hexagonal system and can be assigned to the Zhang-Rice singlet band seen in the hole-doped high-T_c cuprates: the transition from O $1s$ to unoccupied O $2p$ (corresponding to $3d^9L \rightarrow 3d^9$) [23]. The band around 1.3 eV seen in the optical absorption of Fig. 2(a) corresponds to the excitation from these $3d^9L$ state. The intensity of oxygen hole band (Zhang-Rice singlet band) in the O $1s$ XAS spectra is comparable to that of the upper Hubbard band after removing the Sb-O contribution which is roughly indicated by the thick solid line in Fig. 2(d).

In $Ba_3CuSb_2O_9$, the CuO_6 octahedra do not share oxygens, while they are directly connected sharing oxygens at their corners in perovskites or high-T_c cuprates. The oxygen holes in the perovskite are shared by two CuO_6 octahedra and become itinerant for relatively low hole concentration, providing the canonical behavior of Cu $2p$ and O $1s$ x-ray absorption spectra of doped cuprates. On the other hand, the oxygen $2p$ holes in $Ba_3CuSb_2O_9$ can be localized, and its Cu $2p$ and O $1s$ x-ray absorption spectra exhibit different behaviors. In order to verify this point, configuration interaction calculation has been performed for a Cu_6O_{36} cluster in which six CuO_6 octahedra are connected by O-O bond and have one oxygen hole. In the cluster, the six CuO_6 octahedra with Cu $3d$ x^2-y^2 orbital and O $2p_\sigma$ orbitals are considered. The calculated results are shown in Fig. 3. Here U_{dd} and U_{cd} are Coulomb interactions between Cu $3d$ states and between the Cu $2p$ core hole and the Cu $3d$ hole, respectively. Δ is the O $2p$-to-Cu $3d$ charge transfer energy, and $pd\sigma$ and $pp\sigma$ are the Slater-Koster parameters. The effect of O $1s$ core hole potential is neglected. The transfer integral between the neighboring CuO_6 octahedra is given by $(pp\sigma - pp\pi)/\sqrt{2}$ [9] which is evaluated assuming $pp\pi = -1/4pp\sigma$.

For the perovskite cuprates, the main peak of Cu $2p$ XAS usually broadens due to the presence of the mixing of $2p^5 3d^{10}L$ final states with d^9L configurations on neighboring octahedra when the d^9 and d^9L initial states are admixed. On the other hand, for $Ba_3CuSb_2O_9$, the transition from d^9L to $2p^5 3d^{10}L$ appears around 1–2 eV higher than the main peak with a reasonable parameter set as shown in Fig. 3(a), indicating that the average concentration of $\sim$1/6 holes per Cu fits the experimental spectra. As for the O $1s$ spectra [Fig. 3(b)], the prepeak or transition from d^9L to d^9 [so-called Zhang-Rice singlet (ZRS) feature] appears about 2–3 eV lower than

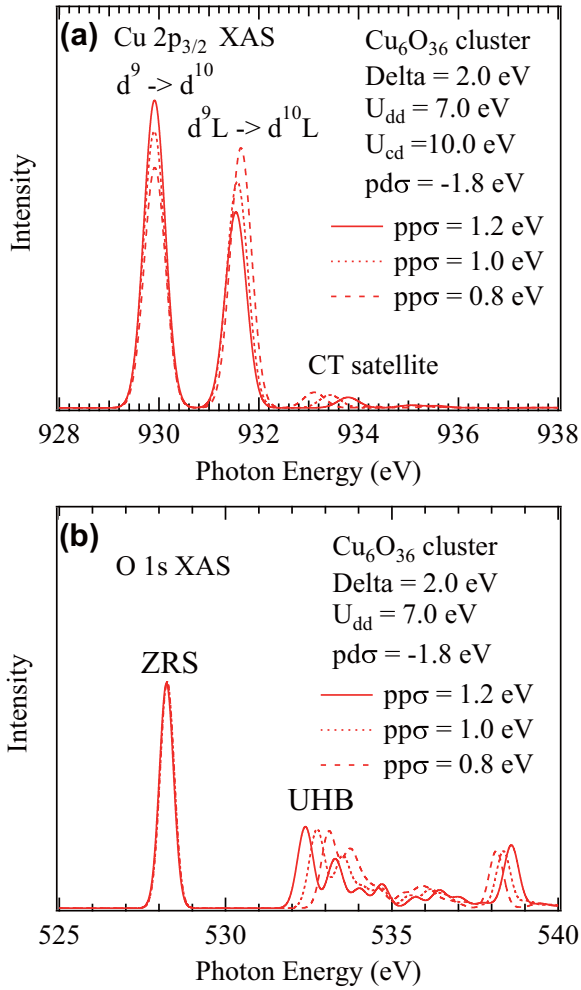

FIG. 3. Configuration interaction calculation for Cu_6O_{36} cluster with one oxygen hole of (a) Cu $2p_{3/2}$ and (b) O 1*s*.

the upper Hubbard band (UHB) peak (the transition to the O 2*p* component mixed into the unoccupied Cu 3*d* level), and is qualitatively consistent with experimental results. The calculated spectral shape is sensitive to the $pp\sigma$ value for the O-O bond which is uncertain. Therefore, it is difficult to determine the hole concentration from the analysis. However, in addition to the qualitative agreement between the observed spectra and the calculated results, the difference of the Sb/Cu ratio between the hexagonal and orthorhombic systems suggests that the hole concentration per Cu site (or Sb2) site is around 1/6.

The presence of the oxygen 2*p* hole in the hexagonal phase indicates that the Cu 3*d* spin and orbital are disturbed by hopping of the oxygen 2*p* holes. The spin and orbital orderings are more strongly suppressed if the systems have more holes. However, it is rather difficult to keep the insulating behavior with oxygen holes. Here we speculate that the amount of 1/6 is important to keep the insulating behavior. Since the hexagonal system with oxygen holes remains highly insulating, these holes should be confined within several Cu sites and disturb the Cu 3*d* spin and orbital of those Cu sites. One of the possible units of confinement is the hexagonal cluster in Fig. 1(b) where the six CuO_6 octahedra are connected through the Cu-O-O-Cu pathways. In this cluster, the oxygen hole and Cu 3*d* spins/orbitals form a quantum object keeping the hexagonal symmetry.

There are several possible origins of the oxygen holes in $Ba_3CuSb_2O_9$. The most plausible possibility is the high valence Sb in the Cu-Sb dimers. The formal valence here is Cu^{2+} and Sb^{5+}. However, the valence state 5+ is rather high for Sb. For such high oxidation states the real electronic configuration tends to contain ligand holes. For example, in $BaBiO_3$ with Bi^{5+}/Bi^{3+} mixed valence, it is established that the formally Bi^{5+} site has the actual electronic configuration close to $Bi^{3+}L^2$ [24]. The same trend is expected for Sb which is located above Bi in the periodic table.

In order to evaluate the valence of the Sb sites, we have carried out the hard x-ray photoemission spectroscopy (HAXPES). Figure 4(a) shows the HAXPES spectra of the hexagonal $Ba_3CuSb_2O_9$. The peak energies of the Sb $3d_{5/2}$ and $3d_{3/2}$ are ~529.9 and ~539.3 eV, respectively, while the Sb $3d_{5/2}$ peak is just overlapped with the O 1*s* peak and thus its energy has uncertainty. These energies are apparently lower than those for the typical Sb^{5+} (or Sb^{4+}) compounds and similar to Sb^{3+} as indicated by the dashed lines in Fig. 4(a). The energies of Sb $3d_{3/2}$, reported on the NIST database including those for Sb_2O_3, Sb_2O_4, Sb_2O_5, and USb_2O_5 [25], are ranging from 539.1 to 540.1 eV for 3+, and 540.1 to 540.8 eV for 5+ (or 4+), respectively. On the other hand, the energies of Sb $3d_{5/2}$ are ranging from 529.2 to 530.1 eV for 3+, and 530.8 to 532.1 eV for 5+ (or 4+), respectively. These results support the suggestion that the actual valence of Sb is close to +3 rather than +5 in the hexagonal phase of $Ba_3CuSb_2O_9$. Therefore, the bonding orbitals constructed from the Sb 5*s* and O 2*p* orbitals have strong Sb 5*s* character and are occupied by electrons while the unoccupied antibonding orbitals have strong O 2*p* character (oxygen 2*p* hole). In the isolated SbO_6 octahedra, the unoccupied antibonding orbitals with O 2*p* character are located within the octahedra, and the localized oxygen 2*p* holes are inactive and are attached to the Sb site, coming back to the formal valence of Sb^{5+}.

On the other hand, in the SbO_6 octahedra in the Cu-Sb dumbbell, the O 2*p* orbitals can be mixed with the Sb 5*s* and Cu 3*d* orbitals since the three oxygens are shared by the SbO_6 and CuO_6 octahedra. In this case, while the bonding orbitals with Sb 5*s* character are occupied by electrons creating Sb^{3+}, the unoccupied antibonding orbitals with O 2*p* character (oxygen 2*p* holes) are extended to the Cu site. If the oxygen 2*p* holes are more strongly bounded to the Sb site than the Cu site, the electronic configuration in the Cu-Sb dimer becomes close to the formal valence of Cu^{2+}-Sb^{5+} which corresponds to the actual valence state of $Cu^{2+}[Sb^{3+}L^2]$ with oxygen 2*p* holes *L*. The oxygen 2*p* holes can be also attached to the Cu site, making the state $[Cu^{2+}L][Sb^{3+}L]$. In the simple schematic picture, the oxygen 2*p* holes may be thus treated as moving in a double-well potential, one well centered on Cu and another, deeper well on Sb, with the barrier in between. The difference between the isolated and the dumbbelled Sb sites manifest in the Sb-O bond length. The average Sb-O bond length is about 2.004 Å in the isolated SbO_6 octahedra while it is about 1.99 Å in the Cu-Sb dumbbell [13]. Consequently, the bond valence sum values [26] for the Sb1 and Sb2 sites are estimated to be 4.81 and 4.35, respectively. Therefore, the Sb2 site accommodates the extra electron to create the oxygen hole.

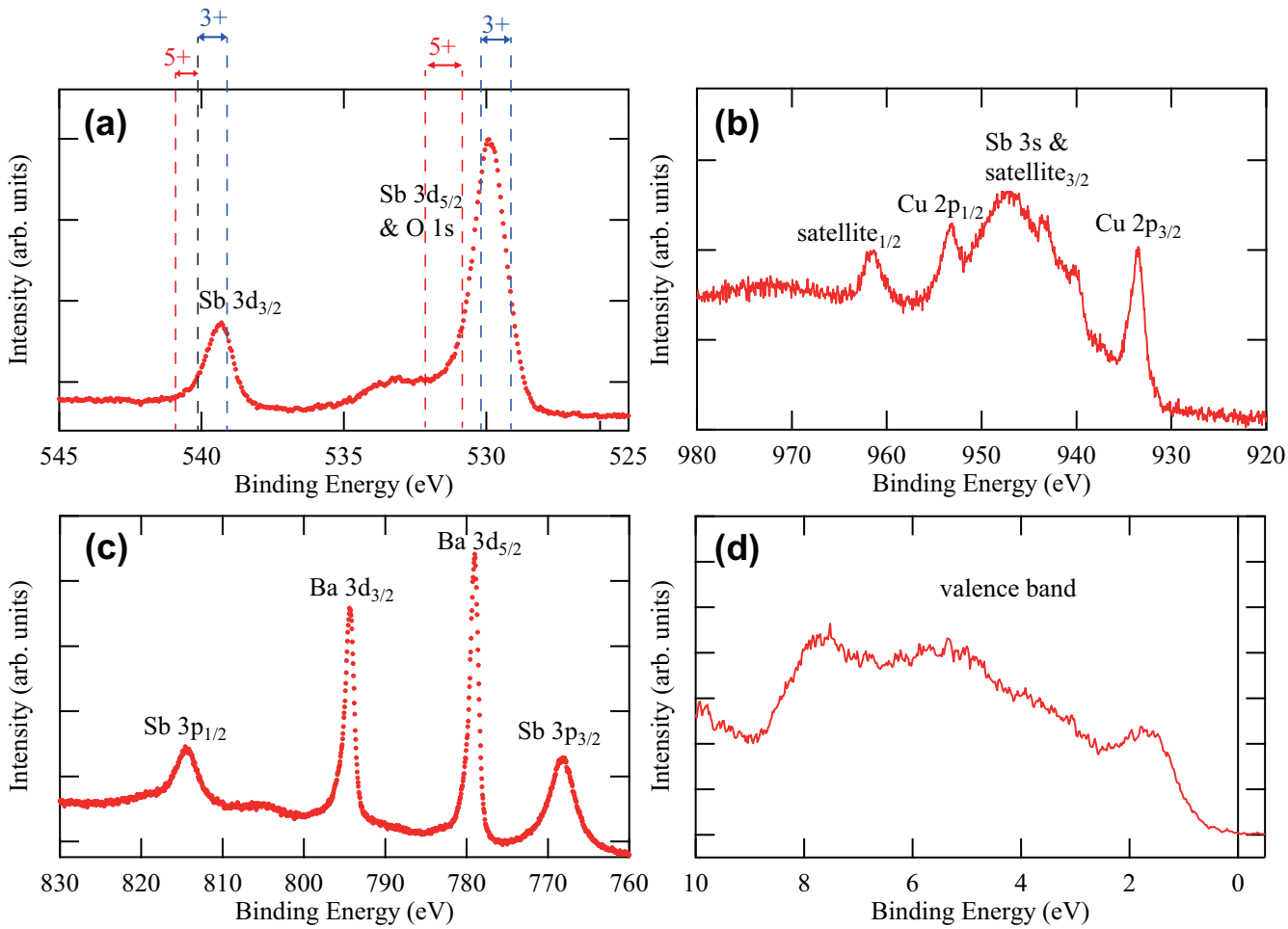

FIG. 4. (a) Sb $3d_{5/2,3/2}$ and O $1s$ HAXPES spectra. The dashed lines indicate the ranges of the binding energy for typical Sb^{3+} and Sb^{5+} compounds reported on the NIST database [25]. (b) Cu $2p_{3/2,1/2}$ and Sb $3s$ HAXPES spectra. (c) Sb $3p_{3/2,1/2}$ and Ba $3d_{5/2,3/2}$ HAXPES spectra. (d) Valence band HAXPES spectrum.

On the other hand, the quantitative estimation of the valence for the Cu sites was hard from the HAXPES spectrum, since the broad Sb $3s$ peak was overlapped onto the satellite structure for the Cu $2p_{3/2}$ observed between 940 and 950 eV [see Fig. 4(b)]. However, the large and sharp satellite structure for Cu $2p_{1/2}$ observed around 962 eV [2] is still consistent with the scenario of the oxygen hole in the hexagonal phase. It should be noted that we had also tried to measure HAXPES for three pieces of the orthorhombic crystals, but all of them were charged up so that no meaningful spectrum was obtained. This fact is also consistent with the highly insulating (or wide-gapped) behavior of the orthorhombic phase compared to the hexagonal one in the optical spectroscopy.

Fluctuation of oxygen $2p$ holes attached either to Sb or to Cu could be the reason of suppression of the long-range Jahn-Teller ordering of Cu in the hexagonal phase. This is the main physics we deduce from our experimental data, which, in our opinion, can explain the main features of the unexpected behavior of $Ba_3CuSb_2O_9$. But even regardless of the origin of the oxygen $2p$ hole, the present results rigorously prove that the oxygen $2p$ hole and the Cu spins form the unique quantum object with spin-charge-orbital fluctuations of the specific time scale in the hexagonal phase. The Cu deficiency or the partial substitution of Cu by Sb was reported for the orthorhombic phase [13]. If one Cu^{2+} is replaced by Sb^{5+}, three oxygen $2p$ holes would be eliminated. Therefore, the oxygen $2p$ holes are removed from the system due to the off-stoichiometry, and the Jahn-Teller distortion is recovered in the orthorhombic phase. This picture is indeed consistent with the O $1s$ XAS spectra in Fig. 2.

It is known that oxygen $2p$ holes play a significant role in high valence transition-metal oxides such as Cu^{3+}, Ni^{3+}, and Fe^{4+} oxides. High valence transition-metal oxides with 90 degrees M-O-M bonds are insulating since the oxygen $2p$ hole mixed with the M $3d$ e_g hole in a MO_4 or MO_6 cluster cannot hop to neighboring clusters and is confined in the single-site cluster [2]. On the other hand, high valence transition-metal oxides with almost 180° M-O-M bonds are metallic and their oxygen $2p$ holes are highly itinerant. With decreasing the M-O-M bond angle in $RNiO_3$ (R = rare earth metal) or $AFeO_3$ (A = alkaline earth metal) by reducing radius of the R or A ions, oxygen $2p$ holes and transition-metal spins are ordered and form spin-charge ordered insulating states [7,27]. Compared to these other oxygen $2p$ hole states in high valence transition-metal oxides, the oxygen $2p$ hole state in $Ba_3CuSb_2O_9$ is very unique in that due to a specific crystal structure with rather

isolated CuO_6 octahedra, the oxygen $2p$ holes have weaker tendency to become itinerant (even with large concentration of oxygen $2p$ holes the hexagonal samples of $Ba_3CuSb_2O_9$ remain highly insulating). This can also lead to a significant difference of XAS spectra in this system as compared, e.g., with the high-T_c cuprates.

In conclusion, x-ray and optical absorption experiments on $Ba_3CuSb_2O_9$ reveal that the hexagonal phase with spin and orbital liquid is characterized by emergence of oxygen $2p$ holes in the highly insulating state. Their appearance originates due to tendency of Sb^{5+} to change electronic state by creating oxygen holes. Oxygen $2p$ holes may fluctuate between Sb and Cu ions, or may be confined in the relatively large hexagonal cluster with six Cu sites, and the CuO_6 JT distortion and long-range magnetic ordering are suppressed due to hopping of oxygen $2p$ holes between Cu and Sb and between CuO_6 octahedra. This can be a rather general situation in many materials containing different metal ions with relatively high valence, in which ligand holes can play crucial role in determining their properties. And the method we used—x-ray spectroscopy—can be one of the best methods to unravel interesting physics connected with these phenomena. Our results demonstrate strong interplay between electronic structure with the presence of oxygen holes in systems with unusual valences, and the Jahn-Teller effect, the effect which often plays crucial role in concentrated solids including high-T_c superconducting cuprates, but also in molecular systems and in inorganic chemistry.

ACKNOWLEDGMENTS

We are grateful for fruitful discussions with and support from S. Koshihara and T. Ishikawa. XAS measurements were performed under the approval of Synchrotron Radiation Research Organization, the University of Tokyo (No. 2015A7401, 2018B7577). HAXPES measurements were performed under the approval of SPring-8 (No. 2018B1449). The work of D.I.K. is funded by the Deutsche Forschungsgemeinschaft (DFG, German Research Foundation), Project number 277146847, CRC 1238.

[1] M. Takano, S. Nasu, T. Abe, K. Yamamoto, S. Endo, Y. Takeda, and J. B. Goodenough, Pressure-Induced High-Spin to Low-Spin Transition In $CaFeO_3$, Phys. Rev. Lett. **67**, 3267 (1991).

[2] T. Mizokawa, H. Namatame, A. Fujimori, K. Akeyama, H. Kondoh, H. Kuroda, and N. Kosugi, Origin of the Band Gap in the Negative Charge-Transfer-Energy Compound $NaCuO_2$, Phys. Rev. Lett. **67**, 1638 (1991).

[3] T. M. Rice and L. Sneddon, Real-Space and $\vec{k}$-Space Electron Pairing in $BaPb_{1-x}Bi_xO_3$, Phys. Rev. Lett. **47**, 689 (1981).

[4] C. M. Varma, Missing Valence States, Diamagnetic Insulators, and Superconductors, Phys. Rev. Lett. **61**, 2713 (1988).

[5] D. I. Khomskii, *Transition Metal Compounds* (Cambridge University Press, Cambridge, 2014).

[6] G. A. Sawatzky and R. Green, The explicit role of anion states in high-valence metal oxides, in *Quantum Materials: Experiments and Theory Modeling and Simulation*, Vol. 6, edited by E. Pavarini, E. Koch, J. van den Brink, and G. A. Sawatzky (Verlag des Forschungszentrum, Julich, 2016), pp. 1–36.

[7] T. Mizokawa, D. I. Khomskii, and G. A. Sawatzky, Spin and charge ordering in self-doped Mott insulators, Phys. Rev. B **61**, 11263 (2000).

[8] F. C. Zhang and T. M. Rice, Effective Hamiltonian for the superconducting Cu oxides, Phys. Rev. B **37**, 3759(R) (1988).

[9] S. Nakatsuji, K. Kuga, K. Kimura, R. Satake, N. Katayama, E. Nishibori, H. Sawa, R. Ishii, M. Hagiwara, F. Bridges, T. U. Ito, W. Higemoto, Y. Karaki, M. Halim, A. A. Nugroho, J. A. Rodriguez-Rivera, M. A. Green, and C. Broholm, Spin-orbital short-range order on a honeycomb-based lattice, Science **336**, 559 (2012).

[10] K. I. Kugel and D. I. Khomskii, The Jahn-Teller effect and magnetism: Transition metal compounds, Sov. Phys. Usp. **25**, 231 (1982).

[11] S. V. Streltsov and D. I. Khomskii, Orbital physics in transition metal compounds: New trends, Phys. Usp. **60**, 1121 (2017).

[12] H. D. Zhou, E. S. Choi, G. Li, L. Balicas, C. R. Wiebe, Y. Qiu, J. R. D. Copley, and J. S. Gardner, Spin Liquid State in the $S = 1/2$ Triangular Lattice $Ba_3CuSb_2O_9$, Phys. Rev. Lett. **106**, 147204 (2011).

[13] N. Katayama, K. Kimura, Y. Han, J. Nasu, N. Drichko, Y. Nakanishi, M. Halim, Y. Ishiguro, R. Satake, E. Nishibori, M. Yoshizawa, T. Nakano, Y. Nozue, Y. Wakabayashi, S. Ishihara, M. Hagiwara, H. Sawa, and S. Nakatsuji, Absence of Jahn-Teller transition in the hexagonal $Ba_3CuSb_2O_9$ single crystal, Proc. Natl. Acad. Sci. USA **112**, 9305 (2015).

[14] Y. Ishiguro, K. Kimura, S. Nakatsuji, S. Tsutsui, A. Q. R. Baron, T. Kimura, and Y. Wakabayashi, Dynamical spin-orbital correlation in the frustrated magnet $Ba_3CuSb_2O_9$, Nat. Commun. **4**, 2022 (2013).

[15] Y. Han, M. Hagiwara, T. Nakano, Y. Nozue, K. Kimura, M. Halim, and S. Nakatsuji, Observation of the orbital quantum dynamics in the spin-1/2 hexagonal antiferromagnet $Ba_3CuSb_2O_9$, Phys. Rev. B **92**, 180410(R) (2015).

[16] L. F. Feiner, A. M. Oles, and J. Zaanen, Quantum Melting of Magnetic order Due to Orbital Fluctuations, Phys. Rev. Lett. **78**, 2799 (1997).

[17] Y. Li, Q. Ma, M. D. N. Shi, and F. C. Zhang, SU(4) Theory for Spin Systems with Orbital Degeneracy, Phys. Rev. Lett. **81**, 3527 (1998).

[18] F. Vernay, K. Penc, P. Fazekas, and F. Mila, Orbital degeneracy as a source of frustration in $LiNiO_2$, Phys. Rev. B **70**, 014428 (2004).

[19] J. Nasu, A. Nagano, M. Naka, and S. Ishihara, Doubly degenerate orbital system in honeycomb lattice: Implication of orbital state in layered iron oxide, Phys. Rev. B **78**, 024416 (2008).

[20] A. T. Boothroyd, C. H. Gardiner, S. J. S. Lister, P. Santini, B. D. Rainford, L. D. Noailles, D. B. Currie, R. S. Eccleston, and R. I. Bewley, Localized $4f$ States and Dynamic Jahn-Teller Effect in PrO_2, Phys. Rev. Lett. **86**, 2082 (2001).

[21] K. Takubo, K. Yamamoto, Y. Hirata, Y. Yokoyama, Y. Kubota, S. Yamamoto, S. Yamamoto, I. Matsuda, S. Shin, T. Seki, K. Takanashi, and H. Wadati, Capturing ultrafast magnetic

dynamics by time-resolved soft x-ray magnetic circular dichroism, Appl. Phys. Lett. **110**, 162401 (2017).

[22] T. Sugimoto, T. Mizokawa, H. Wadati, K. Takubo, A. Damascelli, T. Z. Regier, G. A. Sawatzky, N. Katayama, H. Sawa, K. Kimura, and S. Nakatsuji, X-ray photoemission and x-ray absorption spectroscopy of hexagonal $Ba_3CuSb_2O_9$, JPS Conf. Proc. **1**, 012122 (2014).

[23] C. T. Chen, F. Sette, Y. Ma, M. S. Hybertsen, E. B. Stechel, W. M. C. Foulkes, M. Schulter, S.-W. Cheong, A. S. Cooper, L. W. Rupp, Jr., B. Batlogg, Y. L. Soo, Z. H. Ming, A. Krol, and Y. H. Kao, Electronic States in $La_{2-x}Sr_xCuO_{4+\delta}$. Probed by Soft-X-Ray Absorption, Phys. Rev. Lett. **66**, 104 (1991).

[24] K. Foyevtsova, A. Khazraie, I. Elfimov, and G. A. Sawatzky, Hybridization effects and bond disproportionation in the bismuth perovskites, Phys. Rev. B **91**, 121114(R) (2015).

[25] NIST X-ray Photoelectron Spectroscopy Database, Version 4.1, http://srdata.nist.gov/xps/ (National Institute of Standards and Technology, Gaithersburg, MD, 2012).

[26] R. C. Palenik, K. A. Abboud, and G. J. Palenik, Bond valence sums and structural studies of antimony complexes containing Sb bonded only to O ligands, Inorg. Chim. Acta **358**, 1034 (2005).

[27] V. Bisogni, S. Catalano, R. J. Green, M. Gibert, R. Scherwitzl, Y. Huang, V. N. Strocov, P. Zubko, S. Balandeh, J.-M. Triscone, G. Sawatzky, and T. Schmitt, Ground-state oxygen holes and the metal-insulator transition in the negative charge-transfer rare-earth nickelates, Nat. Commun. **7**, 13017 (2016).